Saral GDR
Quality Assessment Report

Cycle 016

21-08-2014 / 25-09-2014

Prepared by :	S. Philipps , CLS P. Prandi , CLS V. Pignot , CLS JC. Poisson , CLS	
Accepted by :	DT/AQM , CLS	
Approved by :	A. Guillot , CNES	

SALP-RP-P2-EA-22250-CLS016
Edition 01.1, November 2014

1. Introduction

1.1. Document overview

The purpose of this document is to report the major features of the data quality from the Saral/AltiKa mission. The document is associated with data dissemination on a cycle per cycle basis.
This document reports results from Saral/AltiKa GDRs (ocean data).

The objectives of this document are :

To provide a data quality assessment
To provide users with necessary information for data processing
To report any change likely to impact data quality at any level, from instrument status to software configuration
To present the major useful results for the current cycle

1.2. Software version

This cycle has been produced with the following Processing Software references :
L1 library=V4.2p1, L2 library=V5.2p1, Processing Pilot=4.1p1
The results presented in this report have been performed with GDR products in version T (using patch2). **Several flags or algorithms are not yet tuned and have to be used with caution.** A detailed description of the products can be found in the Saral/AltiKa user handbook ([1]). The details of patch2 are listed in **section Content of Patch2**.

1.3. Cycle quality and performances

Data quality for this cycle is nominal.
Analysis of crossovers and sea surface variability indicate that system performances are close to usual values that are obtained from Jason-2 data. For this cycle, the crossover standard deviation is 7.54 cm rms. When using a selection to remove shallow waters (1000 m), areas of high ocean variability and high latitudes ($> |50|^{\circ}$) it decreases down to 5.42 cm rms.
The standard deviation of Sea Level Anomalies (SLA) relative to the mean sea surface is 11.99 cm. When using a selection to remove shallow waters (1000 m), areas of high ocean variability and high latitudes ($> |50|^{\circ}$) it lowers to 8.93 cm .

- Performances from crossover differences are detailed in the dedicated **section Crossover statistics**.
- Detailed CALVAL results are presented in **section 3**.
- Note that two inclination maneuvers took place during cycle 6, which brought Saral/AltiKa to the Envisat repeat ground track (inclination around 81.50°).

During this cycle the following events occurred :
- No TM on 2014-09-09 from 01 :02 :30 to 01 :06 :16 and from 01 :09 :25 to 01 :14 :08 (Pass 539) due to the update of MNT onboard parameters
- Station keeping maneuver on 2014-09-12 from 13 :44 :34 to 13 :44 :36 (Pass 640)
- Several platform mispointing events caused by a rise in reaction wheel friction due to movement of lubricant. Largest events are :
1) 2014-09-04 from 09 :44 :24 to 09 :47 :15 (Pass 406)
2) 2014-09-06 from 18 :38 :32 to 18 :41 :55 (Pass 474)
3) 2014-09-14 from 07 :36 :44 to 07 :38 :50 (Pass 690)

1.4. Information about tracking mode

Saral/AltiKa is able to track data with several onboard tracker algorithms : Median, EDP (Earliest Detectable Part) and Diode/DEM. Median mode is similar to the one used by Envisat and for most cycles of Jason-2. EDP tracker should improve the tracker behavior above continental ice surfaces and hydrological zones. The analysis conducted during the commissioning phase concluded that the median mode is better in average. Finally, Diode/DEM mode is a technique using information coming from Diode and a digital elevation model available onboard. It was already tested on Jason-2. For more information about the different onboard tracker algorithms see [4]. The information about the acquisition / tracking mode used is available in the GDR (fields alt_state_flag_acq_mode_40hz and alt_state_flag_tracking_mode_40hz).

During this cycle, Saral/AltiKa used the following acquisition/tracking modes :

- Passes 1 to 1002 : DIODE acquisition / median tracking

2. Data coverage and edited measurements

This section presents results that illustrate data quality during this cycle. These verification products are produced operationally so that they allow long term monitoring of missing and edited measurements.

2.1. Missing measurements

This cycle has no missing pass, but pass 539 is partially missing with 15.95% of missing ocean data due to the update of onboard parameters.
Missing measurements relative to a nominal ground track are plotted on figure 1.

The map below illustrates missing 1Hz measurements in the GDRs, with respect to a 1Hz sampling of a nominal repeat track. Missing measurements occur over land, especially regions with high relief. This is related to altimeter tracking performances over sloping terrain.

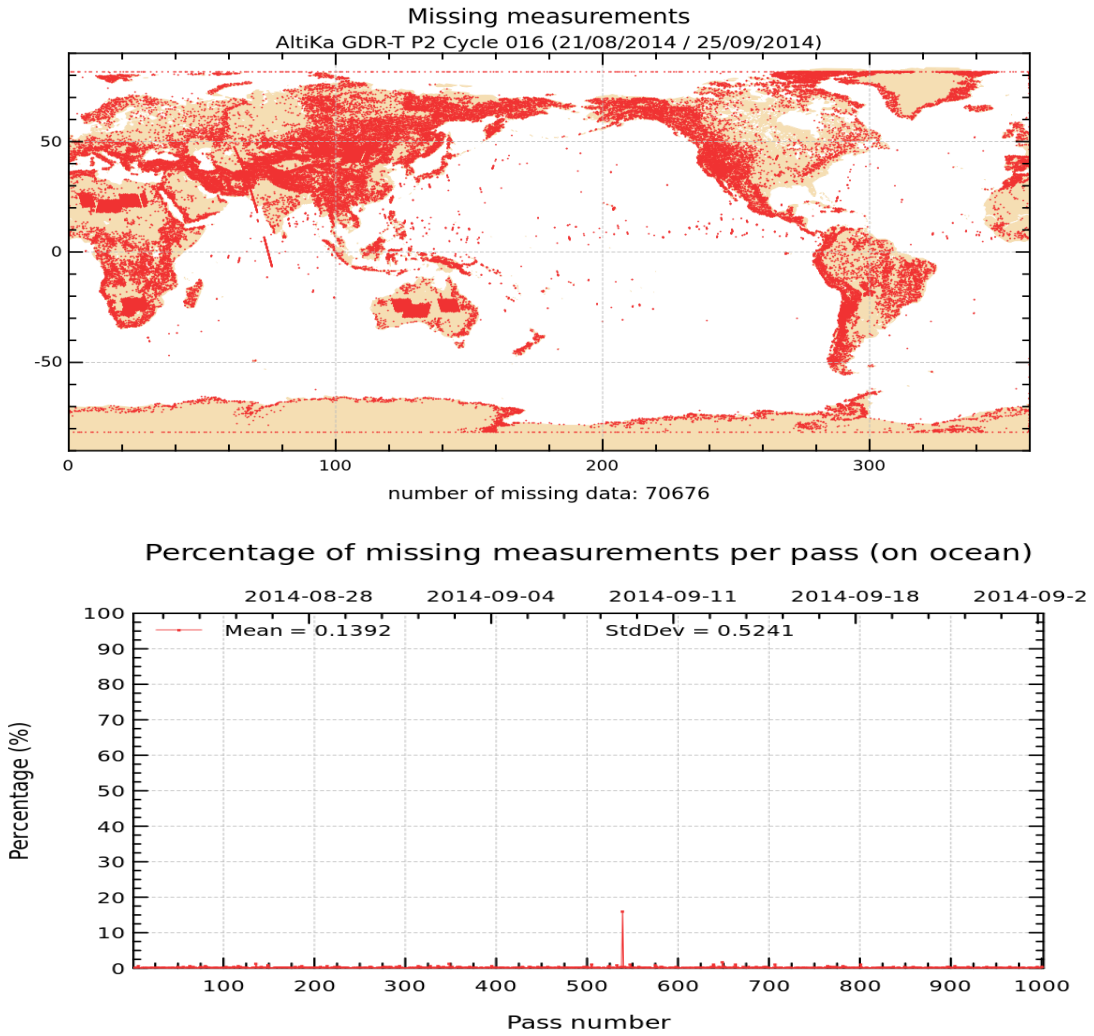

FIGURE 1 – *Map of missing measurements for cycle 016 on top. Monitoring of percentage of missing ocean measurements per pass on bottom*

2.2. Edited measurements

Editing criteria are defined for the GDR product in Saral/AltiKa Product Handbook [1].
The editing criteria are defined as minimum and maximum thresholds for various parameters. Measurements are edited if at least one parameter does not lie within those thresholds. These thresholds are expected to remain constant throughout the Saral/AltiKa mission, so that monitoring the number of edited measurements allows a survey of data quality.
In the following, only measurements over ocean are kept. This is done by keeping only data with surface_type=0 (as well as the Caspian Sea). There is no impact on global performance estimations since the more significant results are derived from analyses in open ocean areas.

The number and percentage of points removed by each criterion is given on the following table. Note that these statistics are obtained with measurements already edited for ice flag ice_flag (17.18 % of points removed).

Parameters	Min threshold	Max threshold	Unit	Nb removed	% removed	% mean removed
Sea surface height	-130	100	m	7118	0.44	0.47
Sea level anomaly	-2	2	m	12363	0.77	0.80
Nb measurements of range	20	DV	_	19153	1.19	1.11
Std. deviation of range	0	0.2	m	24113	1.50	1.48
Square off nadir angle	-0.2	0.0625	deg^2	5502	0.34	0.31
Dry tropospheric correction	-2.5	-1.9	m	0	0.00	0.00
Combined atmospheric correction	-2	2	m	0	0.00	0.00
MWR wet tropospheric correction	-0.5	0	m	933	0.06	0.06
Significant wave height	0	11	m	6233	0.39	0.38
Sea State Bias	-0.5	0.0025	m	4501	0.28	0.29
Backscatter coefficient	3	30	dB	5222	0.33	0.34
Nb measurements of sigma0	20	DV	_	17856	1.11	1.04
Std. deviation of sigma0	0	1	dB	15360	0.96	0.93
Ocean tide	-5	5	m	2908	0.18	0.18
Equilibrium tide	-0.5	0.5	m	2844	0.18	0.17
Earth tide	-1	1	m	0	0.00	0.00
Pole tide	-0.15	0.15	m	0	0.00	0.00
Altimeter wind speed	0	30	$m.s^{-1}$	4501	0.28	0.29
Global statistics of edited measurements by thresholds	_	_	_	43229	2.69	2.53

TABLE 1: *Table of parameters used for editing. 'mean removed' computed over 8 cycles.*

The measurements rejected during the editing process are shown in figure 2. They are mainly situated in ice regions and in regions with disturbed sea state.
- Pass 640 is partially edited by several altimeter parameters out of thresholds (maneuver).
- Besides the maneuver, several passes are also partially edited by mispointing values out of maximum threshold due to wheel friction. Only passes with more than 3% of edited values are listed below :
3.42% on pass 406
8.81% on pass 474
3.73% on pass 682
8.71% on pass 690
3.94% on pass 754
- Besides the mispointing events, several passes are also partially edited by significant wave height values out of maximum threshold in the south hemisphere around -50° latitude which is probably due to geophysical reasons. High SWH values are also observed on Jason-2 in the same region. Only passes with more than 3% of edited values are listed below :
3.64% on pass 215
9.77% on pass 442
8.61% on pass 531
8.93% on pass 569
4.34% on pass 621
6.07% on pass 885
5.37% on pass 896

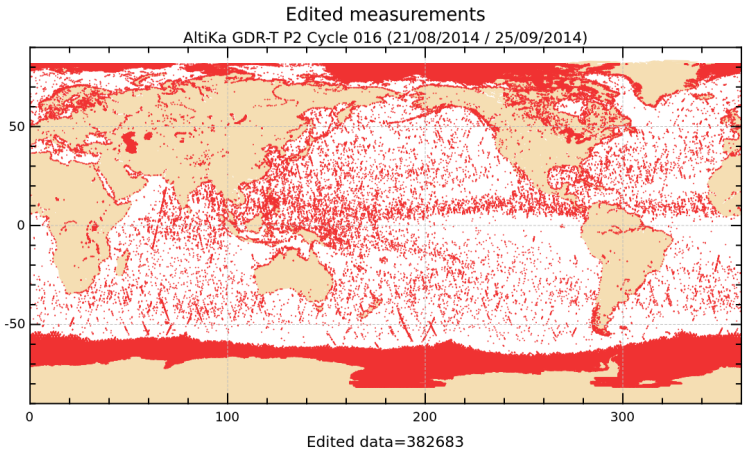

FIGURE 2 – *Edited measurements for cycle 016.*

Map in figure 3 shows the percentage of valid measurements by sample. Wet zones or zones with sea ice appear in the plot as regions with less valid data, as it was also the case for Topex and Jason altimeters : measurements may be corrupted by rain or sea ice. They were therefore removed by editing. There is slightly less data edited on Saral/AltiKa than on Jason-2 mission.

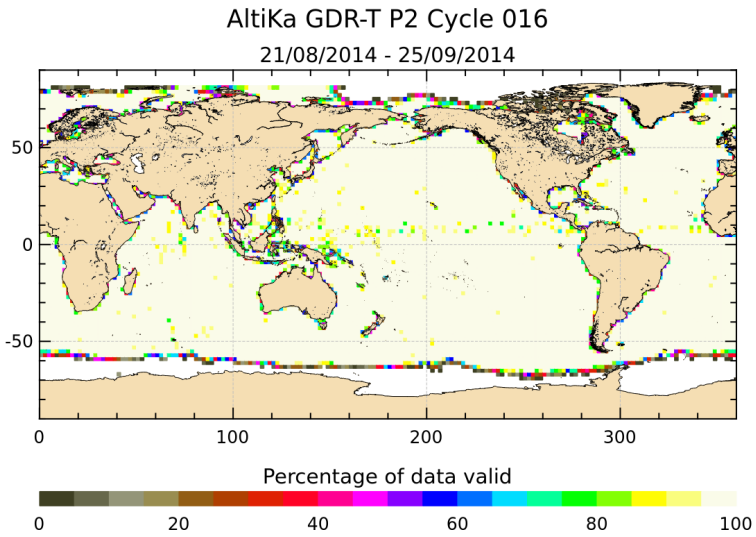

FIGURE 3 – *Percentage of valid measurements for cycle 016. Note that zones, which do not have any valid data (e.g. completely covered by sea ice) are not shown (=white).*

3. Instrumental and geophysical parameter analysis

The monitoring of instrumental and geophysical parameters is crucial to detect potential drifts or jumps in long-term time series. These verification products are produced operationally so that they allow systematic monitoring of the main relevant parameters. When possible, comparison with Jason-2 data are done.

3.1. AltiKa altimeter and sensor

3.1.1. Sensor status

A detailed assessment of the Saral/AltiKa sensor (AltiKa) is made in a separate bulletin, which is available on request ([6]).

3.1.2. AltiKa altimeter status

This section presents the general status of the altimeter for main instrumental variations through the AltiKa mission. Two calibration modes are used to monitor the altimeter internal drifts and compute the altimeter parameters. They are programmed about three times per day, over land (desert areas).
The CAL1 mode measures the Point Target Response (PTR) of the altimeter in Ka-band. Among the parameters extracted from the PTR are :

- the internal path delay
- the total power of the PTR

The evolutions of these parameters as a function of time are plotted to monitor the aging of the altimeter.
The CAL2 mode measures the low pass filter of the altimeter in Ka-band.
Notice that in the Saral/AltiKa products, the range is corrected for the internal path delay and the backscatter coefficient takes into account the total power of the measured PTR.

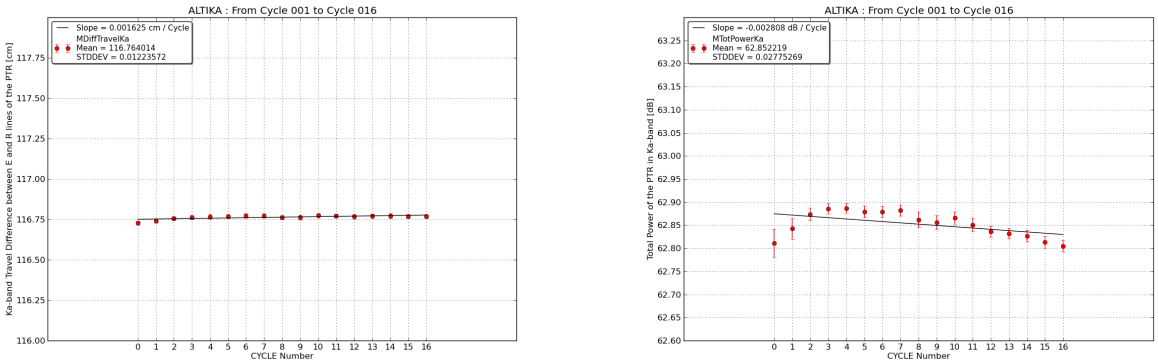

FIGURE 4 – *Internal path delay (left) and total power of the PTR (right) for Ka-band.*

3.2. Significant wave height

Figure 5 shows significant wave height derived from altimeter measurements. Therefore significant wave height data from the current cycle are averaged over a grid of 2° by 2° resolution and smoothed afterwards. Wave height may reach several meters.

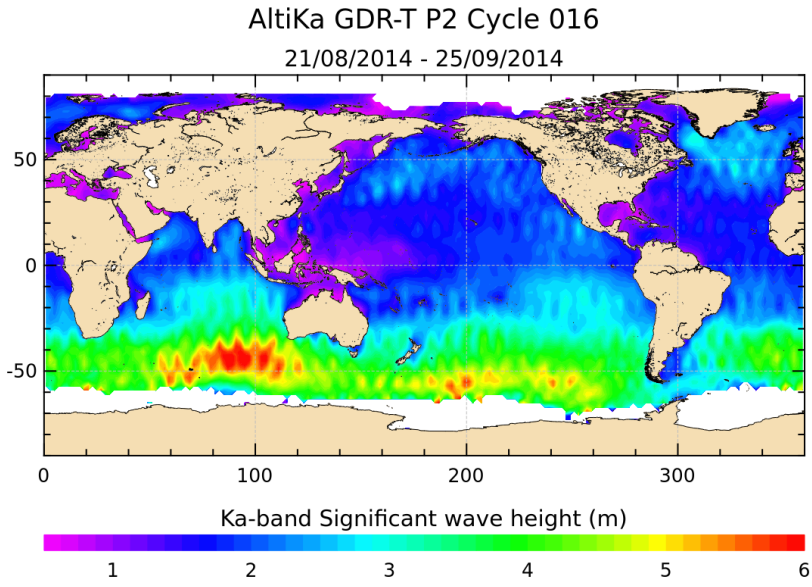

FIGURE 5 – *Significant wave height for cycle 016.*

The daily average of Ku-band SWH for Jason-2 and Ka-band SWH for Saral/AltiKa is plotted as a function of time on figure 6. They show similar features. Note that when computing latitude weighted statistics (not shown here), SARAL/AltiKa significant wave height is generally slightly higher than Jason-2 SWH.

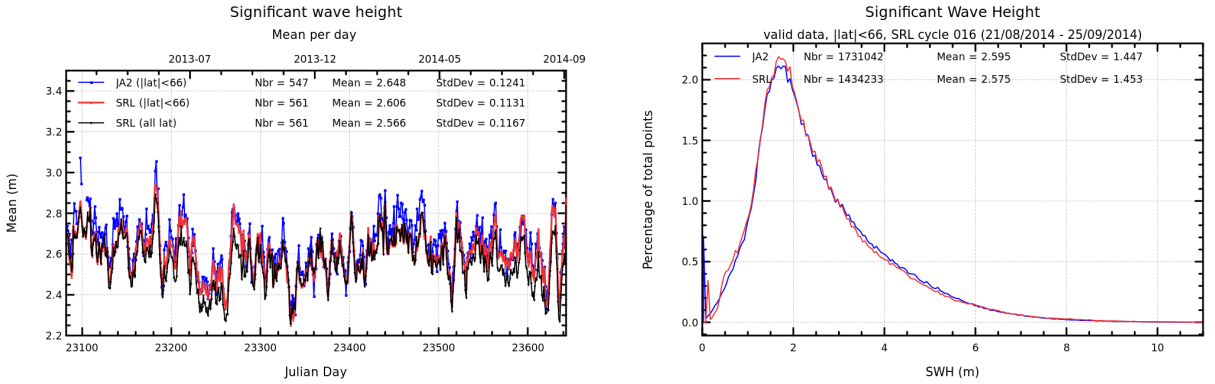

FIGURE 6 – *Daily monitoring of significant wave height for AltiKa (Ka-band) and Jason-2 (Ku-band) on the left and histogram for cycle 016 on the right (limited to 66° latitude).*

3.3. Backscattering coefficient

The daily average of the backscattering coefficient for Saral/AltiKa (Ka-band) and Jason-2 (Ku-band) is plotted as a function of time on figure 7. Note that due to the different frequencies, Saral/AltiKa backscattering coefficient is not simply shifted by a bias, but their histograms have also different forms. Note that the atmospheric attenuation is available in the Saral/AltiKa products and the backscattering coefficient is corrected for it (as it is also done for Jason-2).

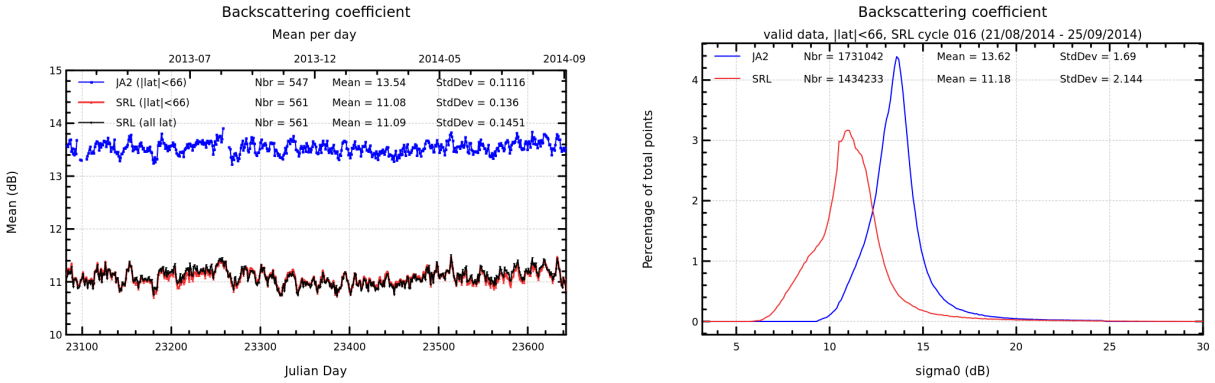

FIGURE 7 – *Daily monitoring of backscattering coefficient for Saral/AltiKa and Jason-2 on the left and histogram for cycle 016 on the right (limited to 66° latitude).*

3.4. Ionosphere correction

As Saral/AltiKa has a mono-frequency altimeter in Ka-band, it is not possible to compute an ionosphere correction derived from altimeter data. Nevertheless considering the frequency, the ionosphere correction in Ka-band is approximately 6 times less than the one in Ku-band. The daily average of dual-frequency ionosphere correction for Jason-2 and GIM ionosphere correction for Saral/AltiKa is plotted as a function of time on figure 8. Note that a scale-factor of $(Frequency_{Ku}/Frequency_{Ka})^2$ was applied to Jason-2 values in this figure, in order to facilitate comparisons between the two missions (though local times and altitude of Jason-2 and Altika data are not the same).

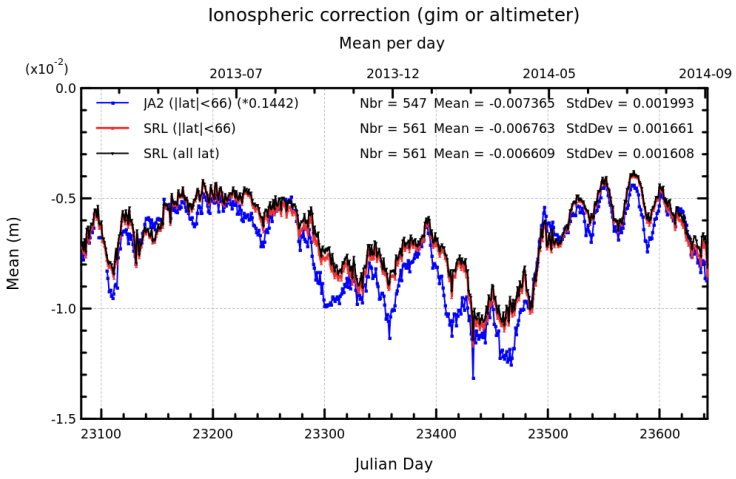

FIGURE 8 – *Daily monitoring of dual-frequency ionosphere correction for Jason-2 and GIM ionosphere correction for Saral/AltiKa.*

3.5. Altimeter wind speed

Figure 9 shows wind speed estimations derived from altimeter measurements. Therefore the data from the current cycle are averaged over a grid of 2° by 2° resolution and smoothed afterwards. Altimeter wind speed for AltiKa GDR-T Patch2 version is estimated with the algorithm of Lillibridge et al. [5], which is based on Abdalla wind speed algorithm [2].

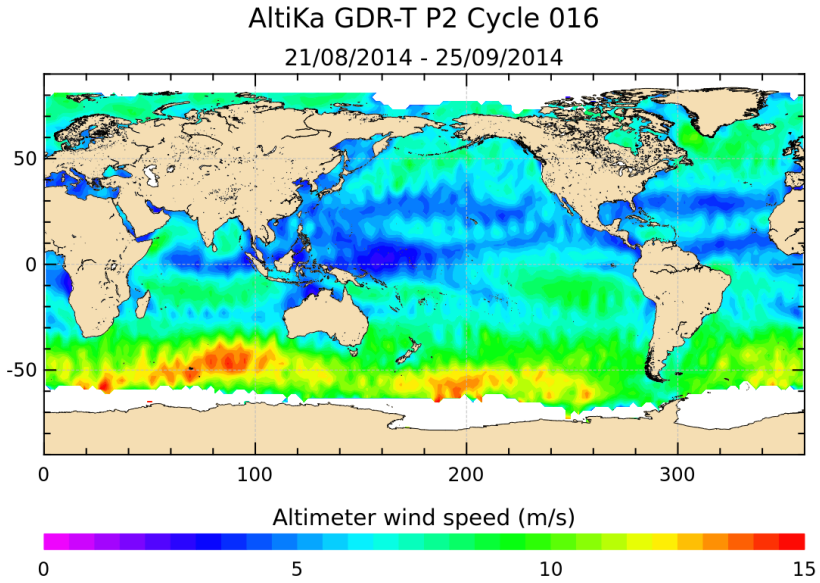

FIGURE 9 – *Altimeter wind speed for cycle 016.*

The daily average of altimeter wind speed for Saral/AltiKa and Jason-2 is plotted as a function of time on the left side of figure 10. The histogram is shown on the right side. AltiKa altimeter wind speed histogram starts around 1 m/s (as other altimeter wind speeds based on Abdalla algorithm). Furthermore a kind of bi-modal behavior is observed (see also [8]). Otherwise, Jason-2 and Saral/AltiKa altimeter wind speeds are similar.

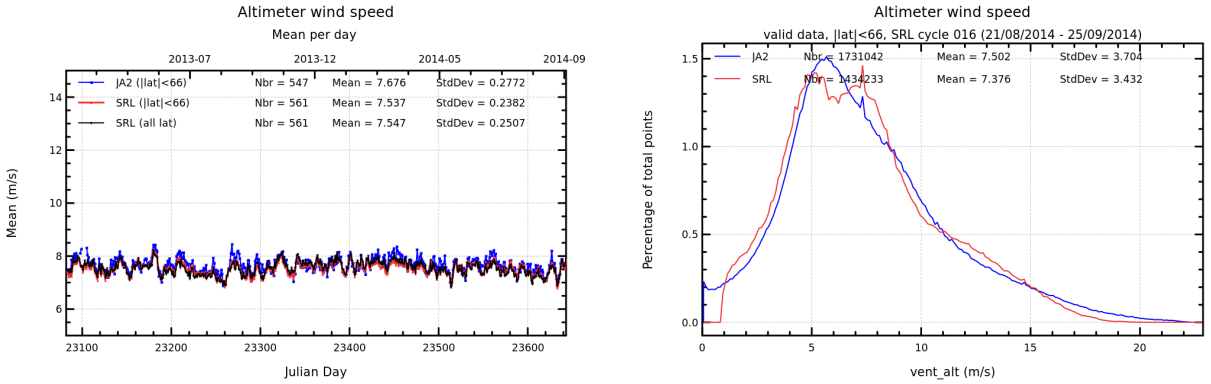

FIGURE 10 – *Daily monitoring of altimeter wind speed for Saral/AltiKa and Jason-2 on the left and histogram for cycle 016 on the right (limited to 66° latitude).*

3.6. Radiometer parameters

The left part of figure 11 shows the mean and standard deviation of wet troposphere correction (radiometer - ECMWF) difference by pass for the current cycle. Beside natural pass to pass variations, there is no anomaly detectable.

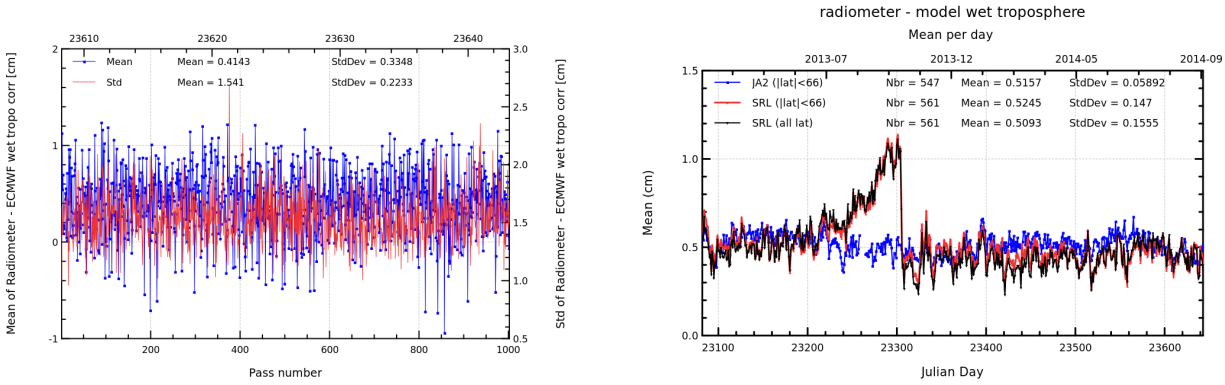

FIGURE 11 – *Pass monitoring of wet troposphere differences between radiometer and ECMWF model for Saral/AltiKa cycle 016 (left) and daily monitoring of wet troposphere differences between radiometer and ECMWF model (right).*

For the current version of the GDR, linear relations have been computed between the measured brightness temperatures and the simulated ones. These linear relations are applied on the 23.8 GHz and 37 GHz channels. Furthermore a bias is applied on sigma0 for computation of the radiometer wet troposphere correction. The radiometer wet troposphere correction is globally quite consistent with the model one, nevertheless the standard deviation of the difference of radiometer minus ECMWF model wet troposphere correction is larger for Saral/AltiKa than for Jason-2 (shown on figure 12), as expected due to the different number of channels (two-frequency radiometer for Saral/AltiKa, three-frequency radiometer for Jason-2) and the new Ka altimeter band used to derive the sea surface roughness. Note that the standard deviation of the wet troposphere difference is already reduced in Patch2 compared to Patch1. Nevertheless work is ongoing to further improve the retrieval algorithms of the radiometer wet troposphere correction .

Note that in summer/fall 2013 (till 2013-10-22), a saturation of the hot calibration counts occurred, which had an impact on the 37 GHz brightness temperature (and the parameters based on it, see right of figure 11). This was not an instrumental problem, but rather an issue related to onboard parameterization.

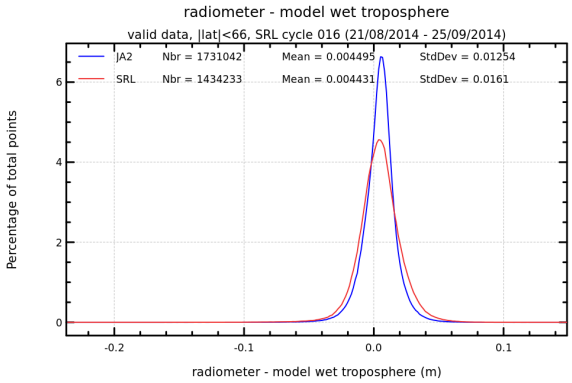

FIGURE 12 – *Histogram of wet troposphere differences between radiometer and ECMWF model for cycle 016.*

4. Crossover Analysis

4.1. Overview

SSH crossover differences are the SSH differences between ascending and descending passes where they cross each other. Crossover differences are systematically analyzed to estimate data quality and the Sea Surface Height (SSH) performances. SSH crossover differences are computed from the valid data set on a one cycle basis, with a maximum time lag of 10 days, in order to limit the effects of ocean variability which are a source of error in the performance estimation. The mean SSH crossover differences should ideally be close to zero and standard deviation should ideally be small.

Nevertheless SLA varies also within 10 days, especially in high variability areas. Furthermore, due to lower data availability (due to seasonal sea ice coverage), models of several geophysical corrections are less precise in high latitude. Therefore an additional geographical selection - removing shallow waters, areas of high ocean variability and high latitudes ($> |50|^{\circ}$) - is applied for cyclic monitoring.

4.2. Maps of SSH crossover differences

The map of the mean differences at crossovers (4 by 4 degrees by bins) is plotted for the current cycle on left panel of figure 13, whereas the right panel shows the whole Saral/AltiKa period.

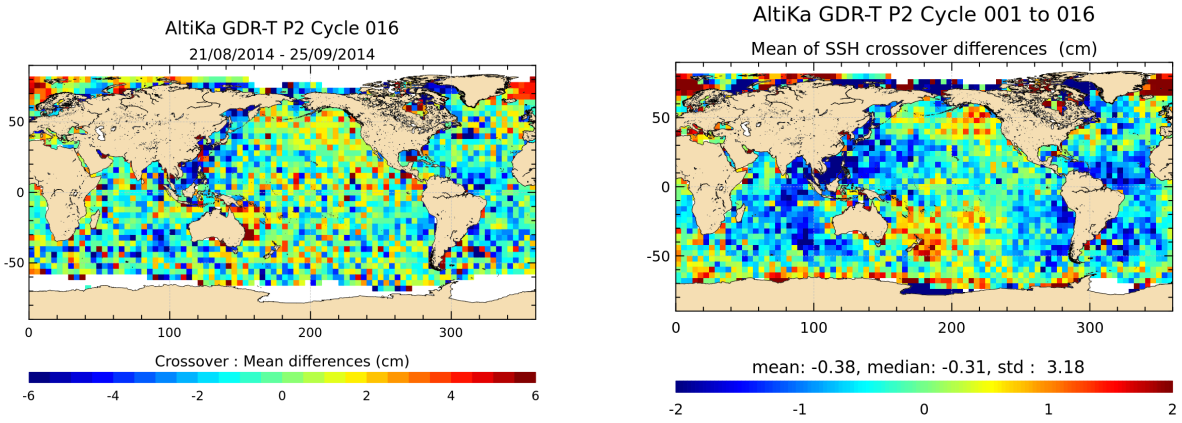

FIGURE 13 – *Mean SSH at crossovers for cycle 016 (left) and over the whole Saral/AltiKa period (right).*

After data editing, applying additional geographical selection (removing shallow waters, areas of high ocean variability and high latitudes ($> |50|^{\circ}$)) and using the standard Saral/AltiKa algorithms, the crossover standard deviation is about 5.42 cm rms.

4.3. Cycle by cycle monitoring

The mean and standard deviation of SSH differences at crossovers are plotted for Saral/AltiKa and Jason-2 as a function of time on a one cycle per cycle basis on top of figure 14. The statistics are computed after data editing and using the geographical selection criteria (|latitude| $< |50|^{\circ}$, bathymetry $< -1000m$, ocean variability (computed over several years) $< 0.2m$). For comparison, statistics of Saral/AltiKa without these selections are also shown in black.
Note that statistics are computed for each cycle based on Saral/AltiKa cycle numbering. Data number may therefore vary between the missions (due to missing or edited measurements). Furthermore figures are computed by averaging in boxes of 4° by 4° resolution and shown on bottom of figure 14. This is done in order to reduce weight of crossover points in high latitudes (there are much more crossover points in high and very high latitudes than in mean and low latitudes, especially for Jason-2).
Saral/AltiKa and Jason-2 show similar performances. Using the radiometer wet troposphere correction improves the coherence between ascending and descending tracks (standard deviation of SSH differences at crossovers points is reduced) for both Jason-2 and Saral/AltiKa. Without box averaging Saral/AltiKa has slightly better performances than Jason-2, with box averages (in order to reduce the weight of the numerous crossover points in high latitudes) Jason-2 has slightly better performances than Saral/AltiKa.

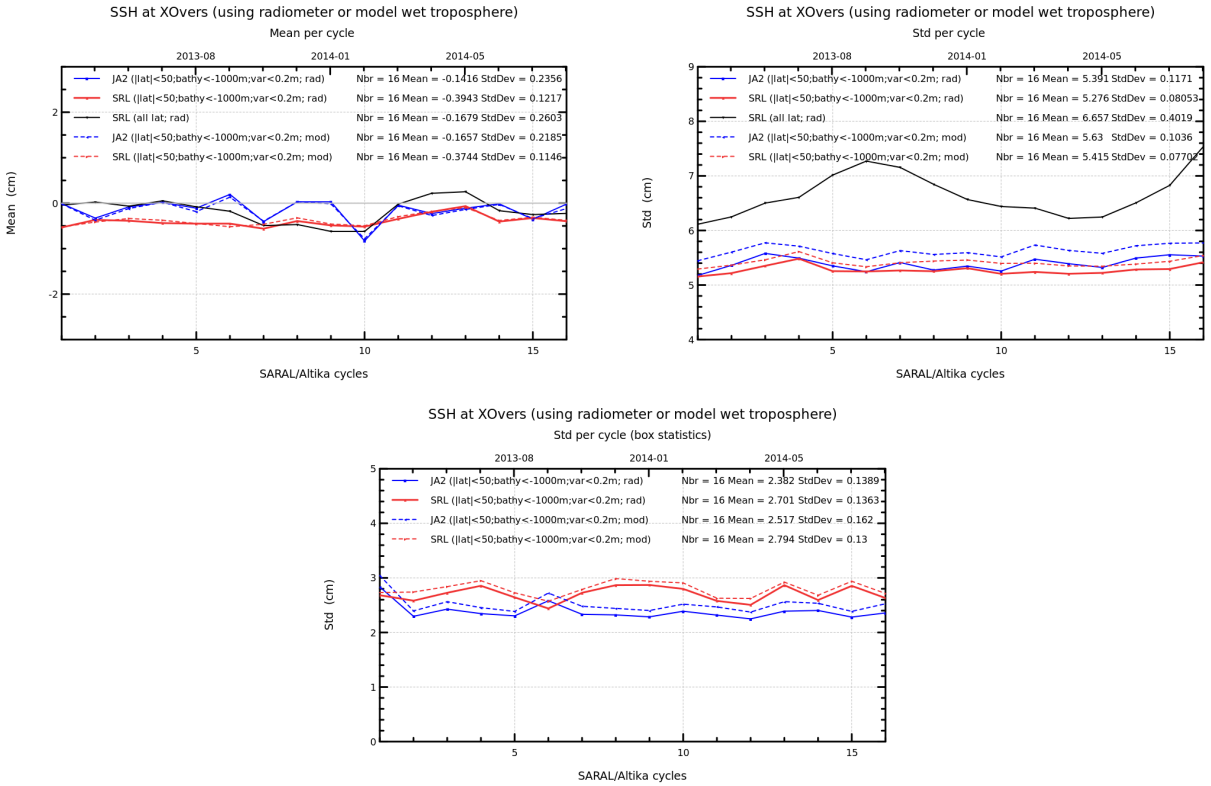

FIGURE 14 – *Cyclic monitoring of mean (left) and standard deviation (right) of SSH differences at crossovers for Saral/AltiKa and Jason-2. Standard deviation of SSH differences at crossover using box averages.*

Figure 15 shows the mean and the standard deviation of Saral/AltiKa − Jason-2 10-days SSH crossovers using radiometer wet troposphere correction or ECMWF model wet troposphere correction for both satellites. The bias between the two missions is close to -4.5 cm when using model wet troposphere correction. Using radiometer wet troposphere correction for both missions reduces the standard deviation at multi-mission crossover points (right of figure 15).

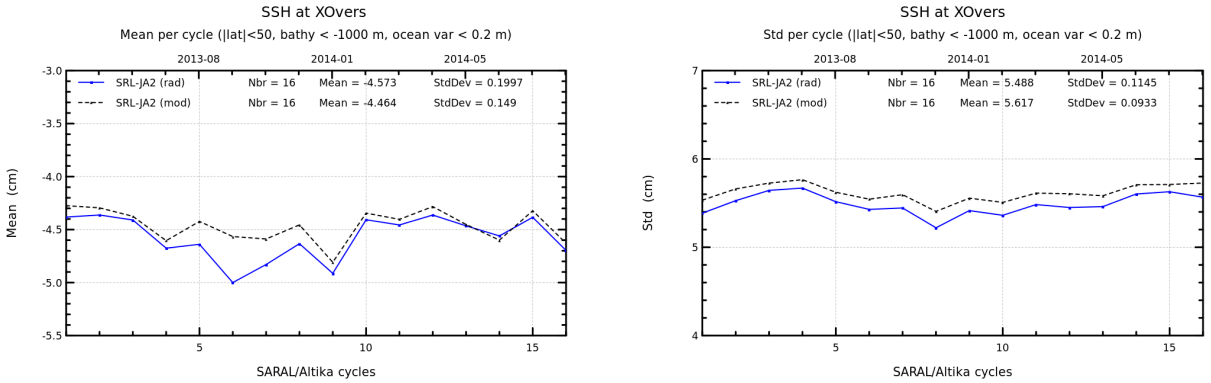

FIGURE 15 – *Cyclic monitoring of mean (left) and standard deviation (right) of (Saral/AltiKa − Jason-2) SSH differences at crossovers using geographical selections.*

4.4. Comparison of pseudo time tag bias

The pseudo time tag bias is found by computing at SSH crossovers a regression between SSH and orbital altitude rate ($\dot{H}$), also called satellite radial speed :

$$SSH = \alpha \dot{H}$$

This method allows us to estimate the time tag bias but it absorbs also other errors correlated with $\dot{H}$ as for instance orbit errors. Therefore it is called "pseudo" time tag bias.

The Jason satellites had a pseudo datation bias close to -0.28 milliseconds with an approximately 60-days signal. The origin of this pseudo time tag bias of the Jason satellites was found by CNES in 2010 [3]. It has a mean of about -0.25 milliseconds and is dependent on the altitude of the satellite. For Jason-2 GDR-D data, the datation was directly modified in order to correct it properly, whereas for Jason-1 GDR-C product it is taken into account thanks to a correction (pseudo_datation_bias_corr_ku). Therefore the average of the pseudo datation bias is now close to zero for the Jason satellites, nevertheless the periodic signal remains and is not yet explained.
Figure 16 shows the monitoring of the pseudo datation bias for Saral/AltiKa and Jason-2 on a cyclic basis (respectively 35 and almost 10 days). Saral/AltiKa shows a small negative pseudo time-tag bias.

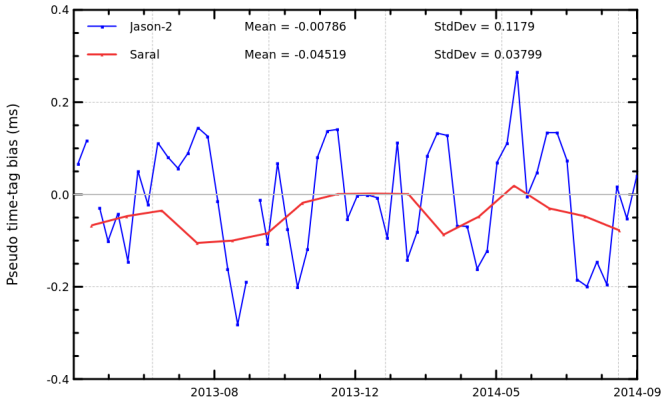

FIGURE 16 – *Cyclic monitoring of pseudo time tag bias for Saral/AltiKa.*

5. Along track analysis

5.1. Mean of along-track SLA

5.1.1. Temporal analysis

The monitoring of mean SLA for Saral/AltiKa and Jason-2 (Figure 17 on left) and the monitoring of mean SLA differences between both missions (Figure 17 on right) is done in order to detect possible jumps or drifts. The bias between both missions is close to -4.5 cm (when using model wet troposphere correction for both missions).

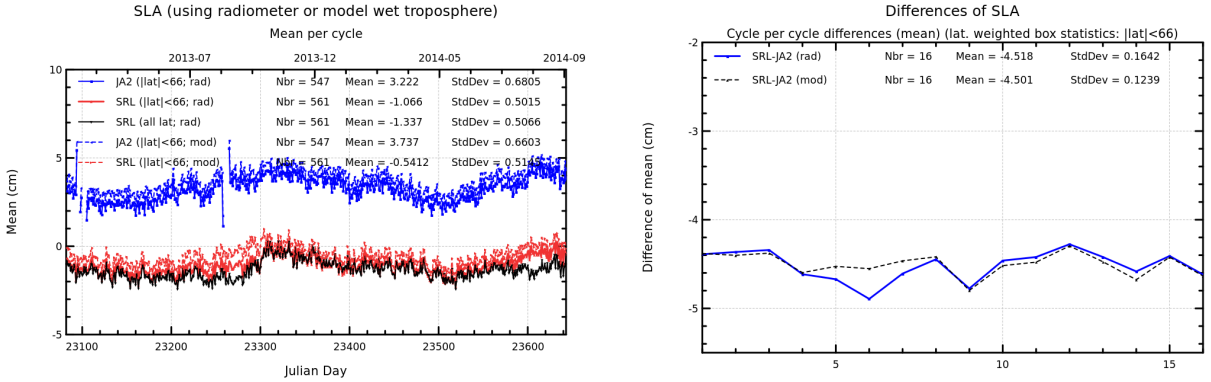

FIGURE 17 – *Daily monitoring of mean SLA for Saral/AltiKa and Jason-2 (left) and cycle per cycle monitoring of differences of (Saral/AltiKa − Jason-2) mean SLA (right).*

5.1.2. Maps

Figures 18 and 19 respectively show the map of Saral/AltiKa SLA relative to the MSS and differences higher than a 30 cm threshold (after centering the data). The latter figure shows that apart from isolated measurements higher differences are located in high ocean variability areas, as expected.

As Saral/AltiKa and Jason-2 are not on the same ground track, maps of direct Saral/AltiKa − Jason-2 SLA measurements are not feasible. But differences of gridded SLA for Saral/AltiKa and Jason-2 can be made. This difference is quite noisy for one cycle (see left of figure 20), sea state changes especially in regions of high ocean variability. Right side of figure 20 shows therefore an average over SLA grid differences from several cycles. High variability regions as Gulf Stream and Antarctic circumpolar current are visible.

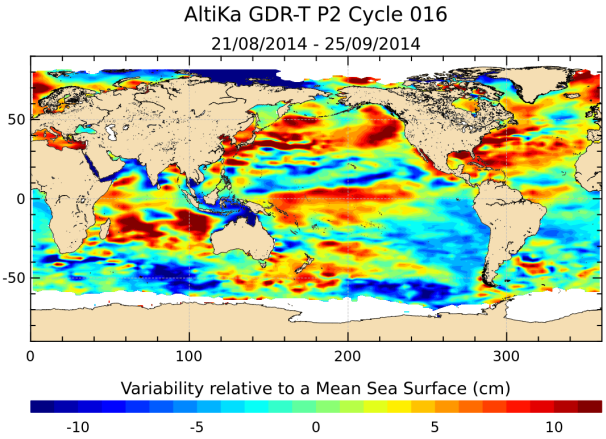

FIGURE 18 – *Sea level anomaly relative to MSS for cycle 016.*

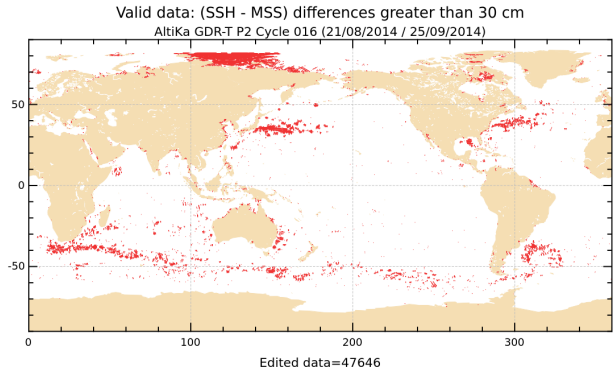

FIGURE 19 – *Differences higher than a 30 cm threshold for cycle 016.*

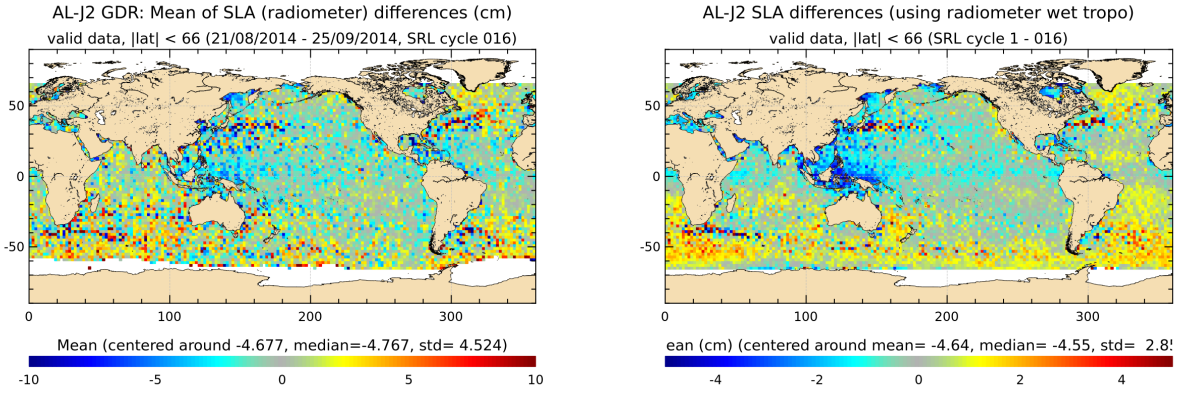

FIGURE 20 – *Saral/AltiKa – Jason-2 SLA differences for cycle 016 (left) and averaged over the whole Saral/AltiKa period (right)*

5.2. Along-track performances

Sea Level Anomaly (SLA) statistics are computed from repeat-track analysis, using radiometer wet troposphere correction. The plot below gives the standard deviation of the SLA for each cycle over the whole data set.

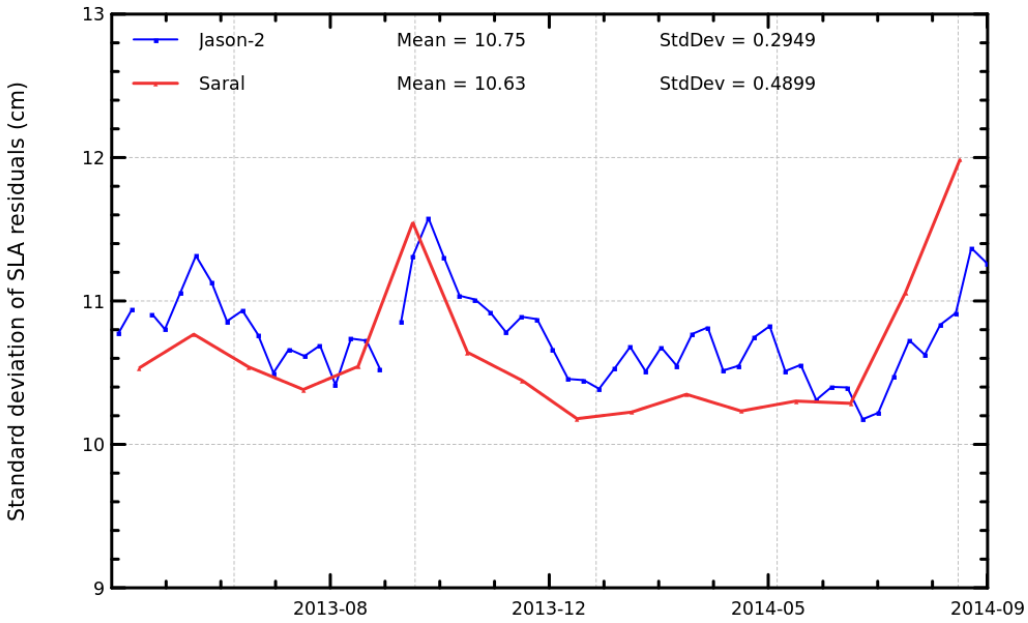

FIGURE 21 – *Cyclic monitoring of standard deviation of along track SLA for Saral/AltiKa and Jason-2 (respectively 35 day and almost 10 day cycles).*

6. Content of Patch1

Hereafter the content of Patch1 is recalled. IGDR data were produced with this patch from cycle 4 pass 395 onwards till cycle 10 pass 565.

Altimeter calibration file : The altimeter calibration stability has been analyzed. Based on the actual data, we have implemented an averaging of the calibrations over a 7 days window for the low pass filter (identical to Jason-2) and 3 days for the internal path delay and total power (not used on Jason-2). This will slightly reduce the daily noise observed in the altimeter calibration data.

Altimeter characterization file : We have updated the altimeter characterization file using the flight calibration of the gain values (4 calibrations performed). The impact is very small (of the order of 0.01 dB).

Retracking look-up tables : We have updated the ocean retracking look-up tables using the flight calibration data (PTR). The impact is very small on the range and sigma0 values but of the order of 15 cms on SWH for low sea states.

MQE : We have analyzed the altimeter flight data and based on the observed MQE values over ocean a threshold of 2.3E-3 (Jason-2 value is 8E-3) is used for the 1Hz data computation.

Neural network : A first linear relation has been computed between the measured BT and the simulated one. This linear relation is applied on the 23.8 GHz only – the same analysis will be conducted on the 37 GHz and sigma0. This generates a bias on the radiometer wet tropospheric correction which is now much more consistent with the model one.

Atmospheric attenuation : The value outputted by the neural algorithm is now recorded in the level2 products (it was set to 0 at the beginning of the mission). Rad_water_vapor and rad_liquid_water : The values have been corrected to comply with the actual unit in the level2 products (kg/m^2). But the rad_liquid_water remains not reliable as an anomaly has been noticed in the neural network.

SSHA : The radiometer wet tropospheric correction is now used to compute this value (the model value was used at the beginning of the mission).

Controls parameters : The threshold values have been updated with the flight data. This is a first tuning – additional work is necessary.

7. Content of Patch2

Hereafter the content of Patch2 is recalled. All GDR data were produced or reprocessed (cycles 1 to 7) with this patch in order to have a homogeneous dataset, whereas IGDR data were only produced with this patch from cycle 10 pass 566 onwards.

Wind look-up table : The table provided by NOAA is used. This table is only based on the measured sigma0, taking into account the atmospheric attenuation (sigma0 at the surface). (Reference : Lillibridge et al. [5])

SSB look-up table : The table provided by R. Scharroo is used (same method as in [7]). We use only the significant wave height to compute the SSB.

Radiometer neural algorithm : Taking into account several months of AltiKa measurements, the neural network coefficients have been updated. Note that this modifies the radiometer related parameters (radiometer wet troposphere correction, atmospheric attenuation, radiometer liquid water content and radiometer water vapor content).

Ice-2 retracking algorithm : The algorithm has been updated taking into account the AltiKa Ka band specificities (ice2 algorithm was based on ENVISAT Ku band experience).

FES2012 tide model : This new tide model is included, improving the SSH accuracy in coastal zones. (Reference : http://www.aviso.oceanobs.com/en/data/products/auxiliary-products/global-tidefes2004-fes99/description-fes2012.html).

Matching pursuit algorithm : The algorithm based on J. Tournadre proposal has been tuned to comply to AltiKa Ka band specificities.

MQE parameter scale factor : The scale factor of the MQE has been modified.

Update of the altimeter characterization file : The altimeter characterization file has been modified in order to account for 63 values of altimeter gain control loop (AGC). This has impacts over sea ice and land hydrology, in some cases the AGC was set to default value in current P1 products.

Doris on ground processing (Triode) : The Doris navigator ground processing has been upgraded to reduce the periodic signal observed on the altitude differences with MOE/POE.

Equilibrium long-period ocean tide height : The equilibrium long-period ocean tide height (ocean_tide_equil) is now at default values over land, but also lakes and inland seas (such as Caspian Sea). Furthermore some ocean data close to land are also at default value. As the geocentric ocean tide height (ocean_tide_sol1) includes ocean_tide_equil, ocean_tide_sol1 is also at default value in the same places as ocean_tide_equil.

Non-equilibrium long-period ocean tide height : The non-equilibrium long-period ocean tide height (ocean_tide_non_equil) of Patch2 is different from the one in Patch1, as it is now computed with FES2012 algorithm, instead of previously FES2004 algorithm.

Références

[1] SARAL/AltiKa Products handbook, December 2013 *SALP-MU-M-OP-15984-CN* edition 2.4. Available at : http://www.aviso.altimetry.fr/fileadmin/documents/data/tools/SARAL_Altika_products_handbook.pdf

[2] Abdalla, S., 2007. Ku-band radar altimeter surface wind speed algorithm. *Proc. of the 2007 Envisat Symposium*, Montreux, Switzerland, 23-27, April 2007, Eur. Space Agency Spec. Publ., ESA SP-636.

[3] Boy, François and Jean-Damien Desjonqueres. 2010. Note technique datation de l'instant de reflexion des échos altimètres pour POSEIDON2 et POSEIDON3 *Reference : TP3-JPOS3-NT-1616-CNES*

[4] J.-D. Desjonqueres, G. Carayon, N. Steunou, and J. Lambin, 2010. Poseidon 3 Radar Altimeter : New Modes and In-Flight Performances. *Marine Geodesy,***33(S1),** 53-79. See : http://www.tandfonline.com/doi/abs/10.1080/01490419.2010.488970#.UjBdPLzCwUE

[5] Lillibridge, J., Scharroo, R., Abdalla, S., and Vandemark, D. (2013) One-and Two-Dimensional Wind Speed Models for Ka-band Altimetry. *Journal of Atmospheric and Oceanic Technology*. doi : http://dx.doi.org/10.1175/JTECH-D-13-00167.1

[6] J. Poisson et al. : AltiKa Instrument Quality Assessment Report Cycle 016. SALP-RP-MA-EA-22233-CLS-016.

[7] Scharroo, R., and J. L. Lillibridge. Non-parametric sea-state bias models and their relevance to sea level change studies, in *Proceedings of the 2004 Envisat & ERS Symposium*, Eur. Space Agency Spec. Publ., ESA SP-572, edited by H. Lacoste and L. Ouwehand, 2005.

[8] R. Scharroo, J. Lillibridge, S. Abdalla, and D. Vandemark. Early look at SARAL/AltiKa data. Oral presentation at OSTST 2013, Boulder, USA. Available at http://www.aviso.altimetry.fr/fileadmin/documents/OSTST/2013/oral/Scharroo_Early_look_at_SARAL.pdf